Electronic Supplementary Material (ESI) for Journal of Materials Chemistry C.

Supporting Information

Fabricating a super stable luminescent chemosensor with multi-stimuli-response to metal ions and small organic molecules by turn-on and turn-off effects

Yan Yang,[a,b] Lian Chen,*[a] Feilong Jiang,[a] Xiuyan Wan,[a,b] Muxin Yu,[a,b] Zhen Cao,[a,b] Tan Jing,[a,b] and Maochun Hong*

[a]*State Key Laboratory of Structure Chemistry, Fujian Institute of Research on the Structure of Matter, Chinese Academy of Sciences, Fuzhou 350002, China.*
[b]*University of the Chinese Academy of Sciences, Beijing, 10049, China*

Contents

Fig. S12 PXRD patterns of the samples before and after the regeneration studies.

Fig. S13 (a) Solid-state luminescent spectra of compound **2** and (b) the luminescence decay curves compound **2** at room temperature.

Fig. S14 Comparison of the $^5D_4 \rightarrow {}^7F_5$ luminescence intensity of **2** in aqueous solutions incorporating different metal ions when excited at 331 nm.

Fig. S15 Comparison of the $^5D_4 \rightarrow {}^7F_5$ luminescence intensity of **2a** introduced into various pure solvent emulsions when excited at 331 nm.

Fig. S16 Comparison of the $^5D_4 \rightarrow {}^7F_5$ luminescence intensity of **2** in the presence of diethyl ether vapour at different times excited at 331 nm.

Fig. S17 Cycles of sensing diethyl ether vapor for compound **2**.

Table S3. Selected bond lengths (Å) and bond angles (º) for compounds **1** and **2**.

Additional Experimental Section

In order to confirm that the mechanism for compound **1** as such a multi-stimuli-responsive sensor of metal ions and small molecules is due to the features of the framework itself, compound **2** ($[Me_2NH_2][TbL(H_2O)]\cdot 1.5H_2O$), the isomorphic structure of compound **1**, was synthesized similarly to **1** except for the use of $Tb(NO_3)_3\cdot 6H_2O$ as starting material. Elemental analysis (%): Calcd for $C_{23}H_{22}TbN_2O_{10.5}$, C, 42.28; H, 3.39; N, 4.29. Found: C, 42.42; H, 3.46; N, 4.35. The PXRD pattern indicates that **1** and **2** are isostructural (Fig. S5).

The CCDC numbers for compound **2** is 1481268. Crystal data and structure refinements for compound **2** are also listed in Table S1, which are available in CIF files in the supporting information.

Table S1. Crystal data and refinement results for compounds **1** and **2**.

	1	**2**
Formula	$C_{23}H_{22}EuN_2O_{10.5}$	$C_{23}H_{22}TbN_2O_{10.5}$
Formula weight	646.39	653.36
Crystal system	monoclinic	monoclinic
space group	C2/c	C2/c
a (Å)	19.6675 (3)	19.6084 (4)
b (Å)	11.9457 (2)	11.9016 (3)
c (Å)	21.9773 (4)	21.9364 (5)
α (°)	90	90
β (°)	97.166 (2)	97.186 (2)
γ (°)	90	90
Volume (Å^3)	5123.06 (15)	5079.1 (2)
T (K)	100	100
Z	8	8
F (000)	2216	2248
R_1 (I>2σ(I))	0.0316	0.0291
wR_2 (reflections)	0.1023	0.0748

[a]$R_1 = \Sigma||F_o| - |F_c||/\Sigma|F_o|$. [b]$\omega R_2 = [\Sigma\omega(F_o^2 - F_c^2)^2/\Sigma\omega(F_o^2)^2]^{1/2}$.

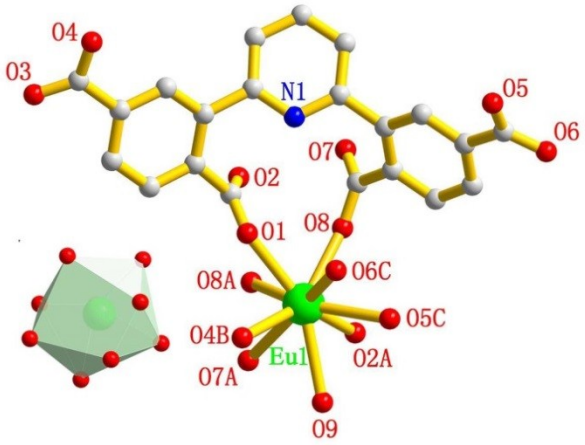

Fig. S1 Coordination environment of the Eu^{3+} ion in compound **1**. All H atoms and solvent molecules are omitted. Inset: coordination polyhedron of Eu^{3+} ion. (Symmetry codes: A, 3/2-*x*, 3/2-*y*, 1-*z*; B, 3/2-*x*, 1/2+*y*, 1/2-*z*; C, 2-*x*, 1-*y*, 1-*z*. Eu^{3+}, green; O, red; N, blue; C, gray).

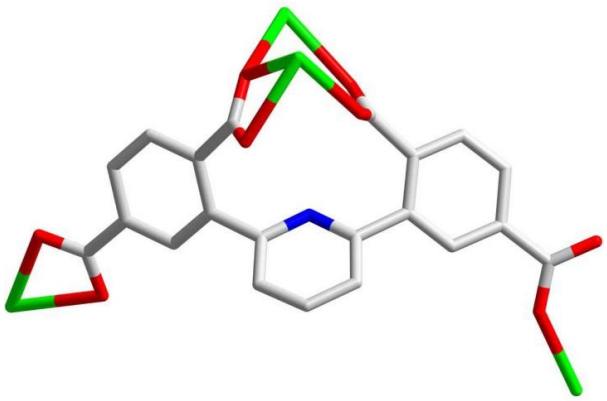

Fig. S2 The coordination mode of $[L]^{4-}$ in **1**: μ_8-bridging mode.

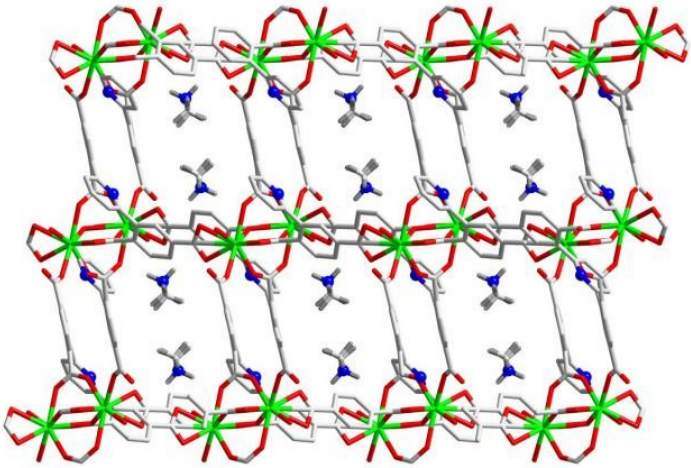

Fig. S3 The encapsulated counter cations $[H_2NMe_2]^+$ in channel A.

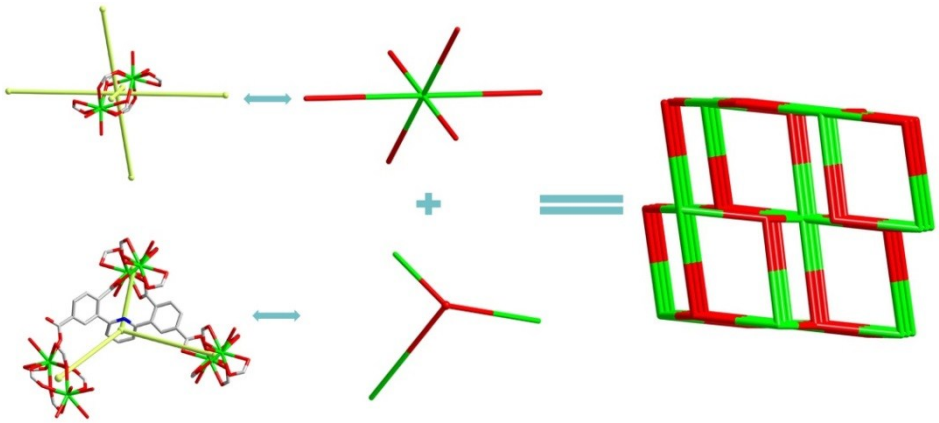

Fig. S4 (a) The simplified 6-connected node of the binuclear unit [$Eu_2(\mu_2$-$COO)_2(COO)_2$]. (b) The simplified 3-connected node of the ligand. (c) The (3, 6)-connected topological two-nodal net with the Schläfli symbol $\{4^2.6\}_2\{4^4.6^2.8^7.10^2\}$ in compound **1**.

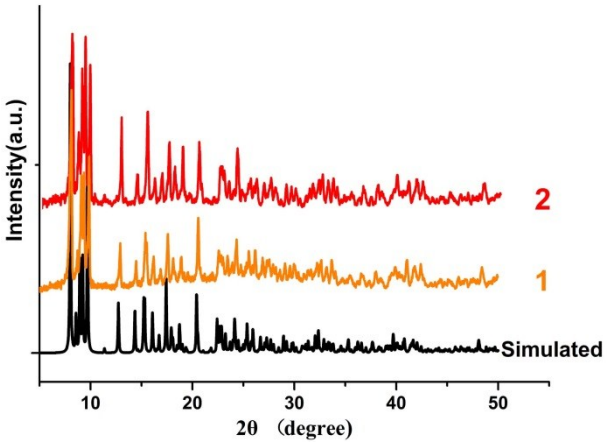

Fig. S5 PXRD patterns of compounds **1** and **2**.

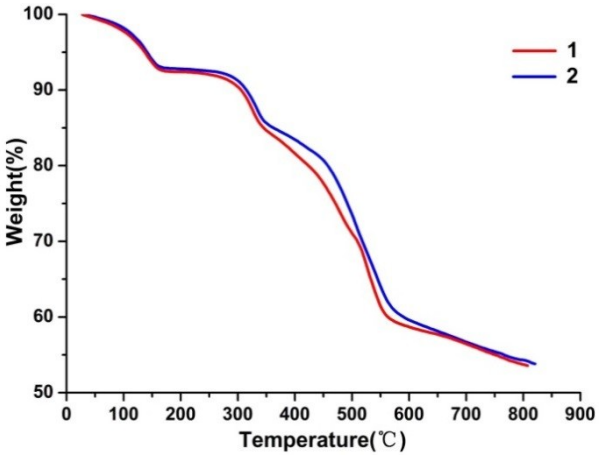

Fig. S6 The TGA curves of compounds **1** and **2**.

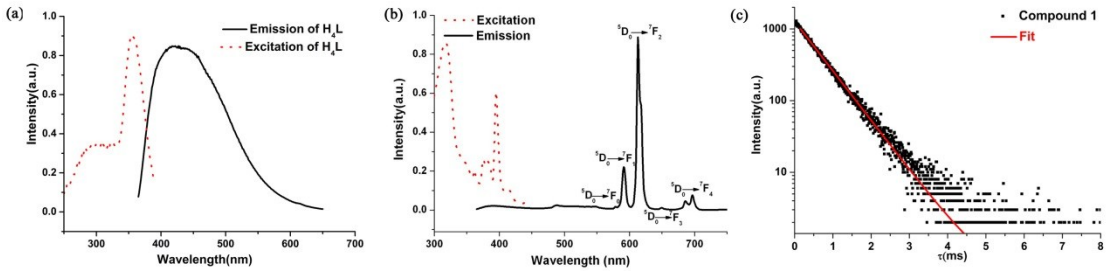

Fig. S7 Room-temperature luminescent spectra of (a) the ligand H_4L (excitation: dot, λ_{em}= 425 nm; emission: solid, λ_{ex}= 350 nm) (b) compound **1** in solid state. (c) The luminescence decay curves compound **1** at room temperature.

Table S2. The ICP results of compound **1** and M^{n+}-**1** (M^{n+} = Na^+, K^+, Cu^{2+}, Zn^{2+}, Cd^{2+}, Ni^{2+}, Mn^{2+}, Pb^{2+}, Mg^{2+}, Co^{2+}, Cr^{3+}, Tb^{3+}, Al^{3+}, Ag^+, Fe^{3+}, respectively)

Compound	Eu^{3+}(wt%)	M^{n+}(wt%)	Compound	Eu^{3+}(wt%)	M^{n+}(wt%)
1	19.03	-	Pb^{2+}-1	16.28	3.98
Cd^{2+}-1	**18.74**	**5.87**	Co^{2+}-1	20.59	0.325
Tb^{3+}-1	18.10	0.84	Na^+-1	17.78	3.03
K^+-1	18.04	3.61	Fe^{3+}-1	17.25	0.55
Ag^+-1	17.44	7.73	Ni^{2+}-1	21.36	0.081
Mg^{2+}-1	18.28	0.0607	Cu^{2+}-1	17.51	1.30
Al^{3+}-1	20.14	0.36	Zn^{2+}-1	19.46	3.00
Cr^{3+}-1	19.80	0.134	**Mn^{2+}-1**	**19.70**	**2.98**

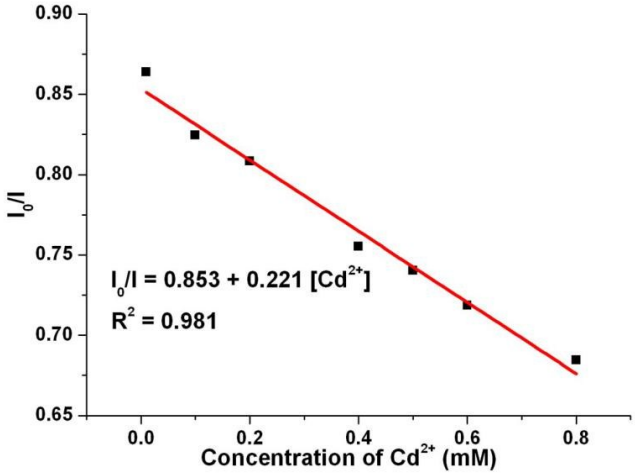

Fig. S8 The Stern-Volmer plot between the enhancing effect and the concentration of Cd^{2+} ions at low concentrations.

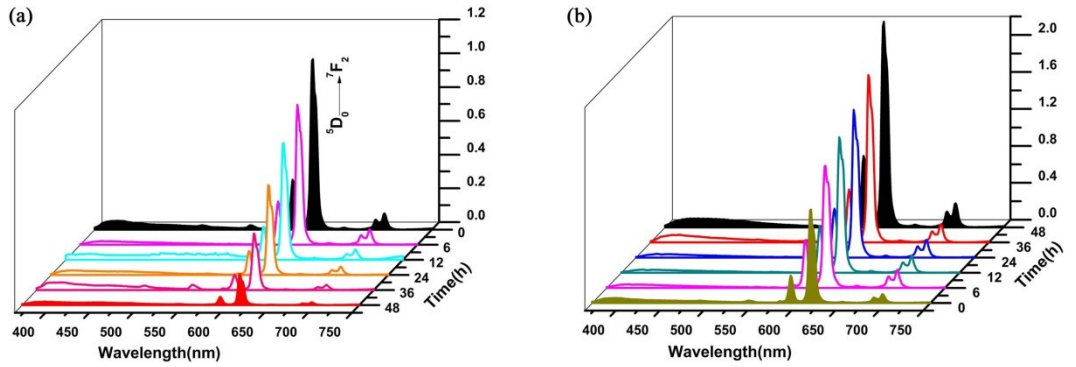

Fig. S9 Comparison of the $^5D_0 \rightarrow {}^7F_2$ luminescence intensity of **1** in aqueous solutions incorporating (a) Mn^{2+} ions and (b) Cd^{2+} ions in different times when excited at 324 nm.

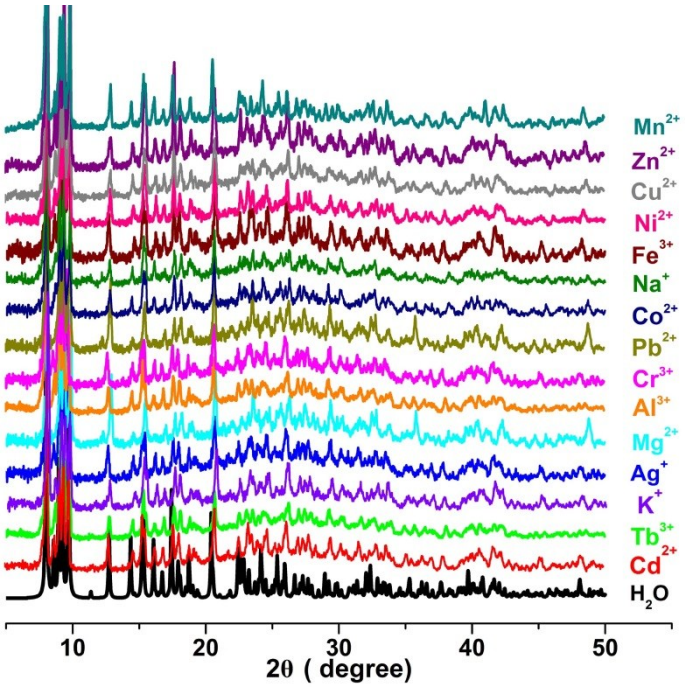

Fig. S10 PXRD patterns of **1** after dispersed in different $M(NO_3)_x$ (x= Na^+, K^+, Cu^{2+}, Zn^{2+}, Cd^{2+}, Ni^{2+}, Mn^{2+}, Pb^{2+}, Mg^{2+}, Co^{2+}, Cr^{3+}, Tb^{3+}, Al^{3+}, Ag^+, Fe^{3+}) in aqueous water solvents.

Scheme S1. Simplified views of the probable luminescent enhancing and quenching mechanisms of compound **1** by Cd^{2+} and Mn^{2+} ions.

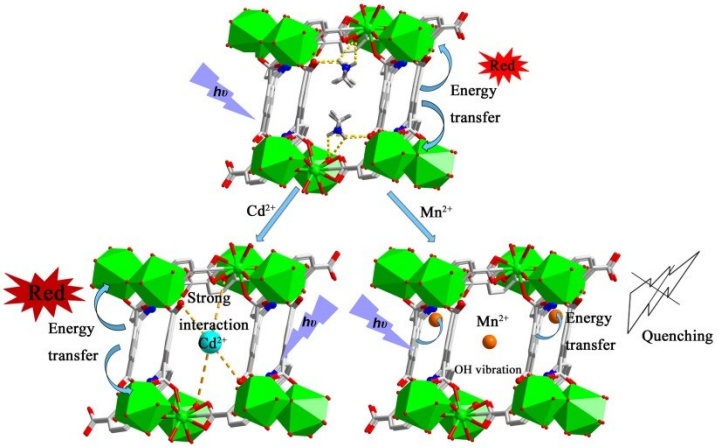

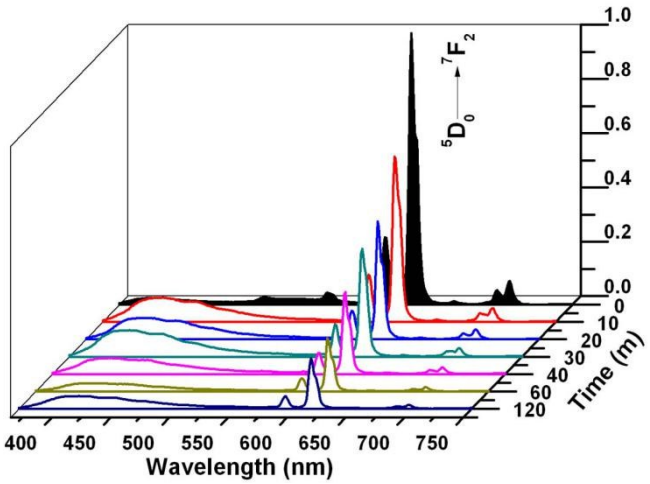

Fig. S11 Comparison of the $^5D_0 \rightarrow {}^7F_2$ luminescence intensity of **1** in the presence of diethyl ether vapour in different times.

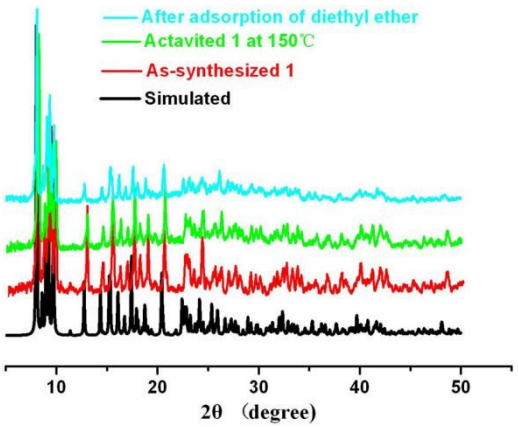

Fig. S12 PXRD patterns of the samples before and after the regeneration studies.

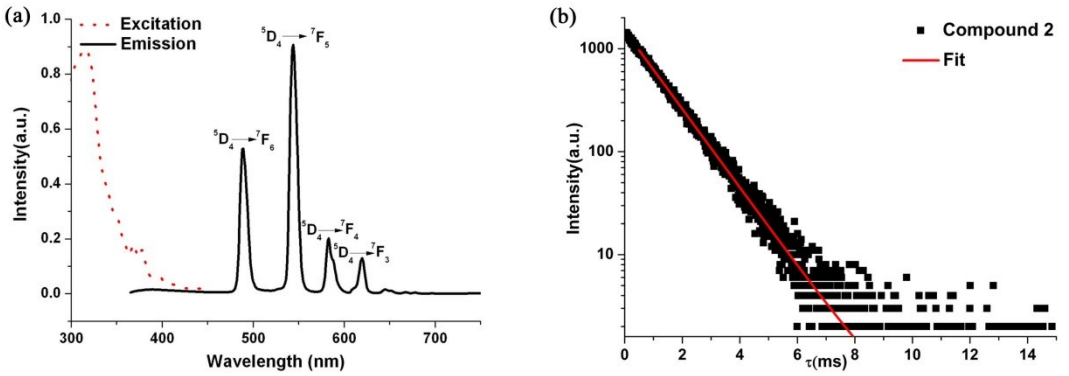

Fig. S13 (a) Solid-state luminescent spectra of compound **2** and (b) the luminescence decay curves compound **2** at room temperature.

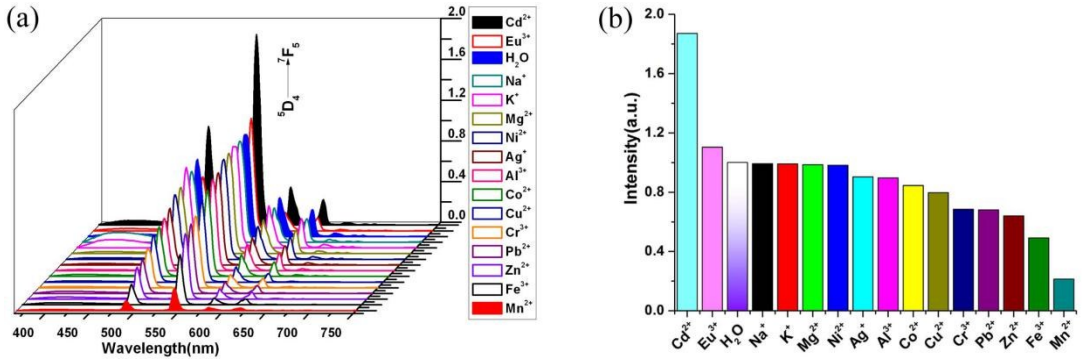

Fig. S14 Comparison of the $^5D_4 \rightarrow {}^7F_5$ luminescence intensity of **2** in aqueous solutions incorporating different metal ions when excited at 331 nm.

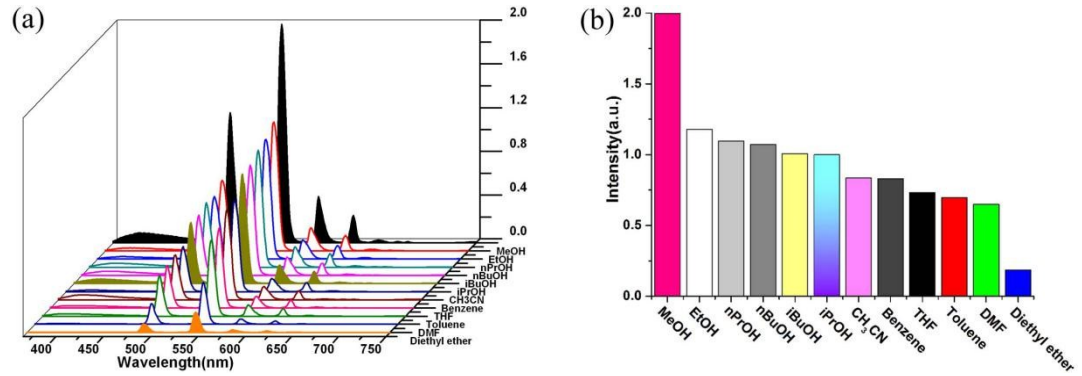

Fig. S15 Comparison of the $^5D_4 \rightarrow {}^7F_5$ luminescence intensity of **2a** introduced into various pure solvent emulsions when excited at 331 nm.

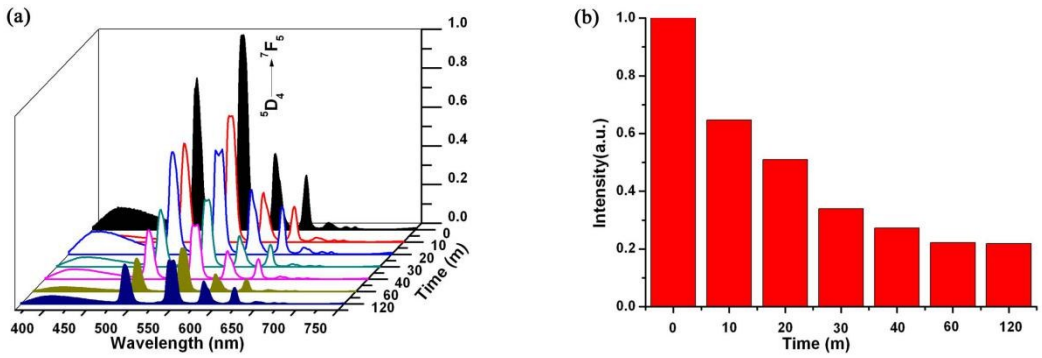

Fig. S16 Comparison of the $^5D_4 \rightarrow {}^7F_5$ luminescence intensity of **2** in the presence of diethyl ether vapour at different times excited at 331 nm.

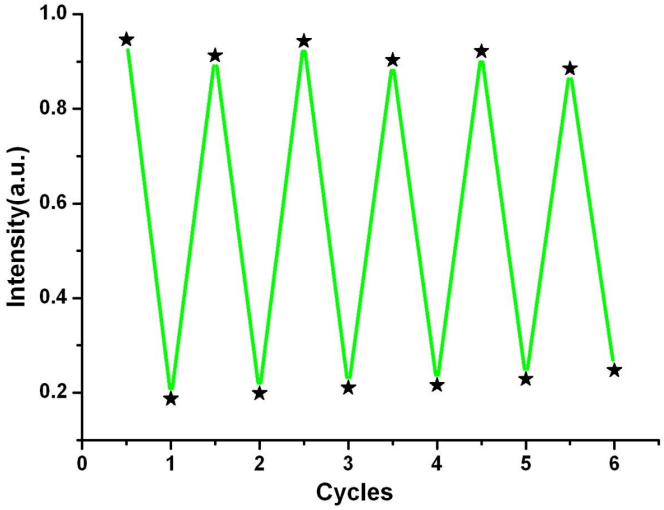

Fig. S17 Cycles of sensing diethyl ether vapor for compound **2**.

Table S3. Selected bond lengths (Å) and bond angles (º) for compounds **1** and **2**.

Bond	Dist.	Bond	Dist.
Eu1—O4^{i}	2.338 (3)	Eu1—O7^{ii}	2.488 (3)
Eu1—O8	2.378 (3)	Eu1—O5^{iii}	2.489 (3)
Eu1—O1	2.383 (3)	Eu1—O9	2.583 (4)
Eu1—O2^{ii}	2.422 (3)	Eu1—O8^{ii}	2.632 (3)
Eu1—O6^{iii}	2.445 (4)		
Angle	(º)	Angle	(º)
O4^{i}—Eu1—O8	146.11 (12)	O2^{ii}—Eu1—O5^{iii}	78.78 (11)
O4^{i}—Eu1—O1	74.27 (12)	O6^{iii}—Eu1—O5^{iii}	52.64 (11)
O8—Eu1—O1	74.16 (11)	O7^{ii}—Eu1—O5^{iii}	134.30 (11)
O4^{i}—Eu1—O2^{ii}	139.60 (12)	O4^{i}—Eu1—O9	75.11 (11)
O8—Eu1—O2^{ii}	73.82 (11)	O8—Eu1—O9	137.46 (11)
O1—Eu1—O2^{ii}	136.40 (11)	O1—Eu1—O9	148.33 (11)
O4^{i}—Eu1—O6^{iii}	77.24 (14)	O2^{ii}—Eu1—O9	68.36 (11)
O8—Eu1—O6^{iii}	83.30 (13)	O6^{iii}—Eu1—O9	105.18 (13)
O1—Eu1—O6^{iii}	75.66 (12)	O7^{ii}—Eu1—O9	65.49 (12)
O2^{ii}—Eu1—O6^{iii}	128.22 (11)	O5^{iii}—Eu1—O9	70.53 (12)
O4^{i}—Eu1—O7^{ii}	75.42 (13)	O4^{i}—Eu1—O8^{ii}	106.37 (12)
O8—Eu1—O7^{ii}	121.59 (11)	O8—Eu1—O8^{ii}	73.63 (12)
O1—Eu1—O7^{ii}	98.83 (11)	O1—Eu1—O8^{ii}	69.89 (10)
O2^{ii}—Eu1—O7^{ii}	74.22 (11)	O2^{ii}—Eu1—O8^{ii}	73.22 (10)
O6^{iii}—Eu1—O7^{ii}	152.57 (12)	O6^{iii}—Eu1—O8^{ii}	142.51 (12)
O4^{i}—Eu1—O5^{iii}	105.05 (13)	O7^{ii}—Eu1—O8^{ii}	50.83 (10)
O8—Eu1—O5^{iii}	83.87 (12)	O5^{iii}—Eu1—O8^{ii}	147.92 (11)
O1—Eu1—O5^{iii}	125.79 (11)	O9—Eu1—O8^{ii}	111.84 (11)

Symmetry codes: (i) 1/2-x, 1/2+y, -1/2-z; (ii) 1/2-x, 1/2-y, -z; (iii) 1-x, -y, -z.

Bond	Dist.	Bond	Dist.
Tb1—O4^{i}	2.326 (2)	Tb1—O7^{ii}	2.457 (2)
Tb1—O8	2.354 (2)	Tb1—O5^{iii}	2.4763 (11)
Tb1—O1	2.354 (2)	Tb1—O9	2.5465 (11)
Tb1—O2^{ii}	2.392 (2)	Tb1—O8^{ii}	2.613 (2)
Tb1—O6^{iii}	2.4149 (10)		
Angle	(º)	Angle	(º)
O4^{i}—Tb1—O8	145.69 (8)	O8—Tb1—O5^{iii}	83.75 (6)
O4^{i}—Tb1—O1	73.74 (8)	O1—Tb1—O5^{iii}	125.68 (6)
O8—Tb1—O1	74.32 (7)	O2^{ii}—Tb1—O5^{iii}	78.56 (6)
O4^{i}—Tb1—O2^{ii}	139.69 (8)	O6^{iii}—Tb1—O5^{iii}	53.1
O8—Tb1—O2^{ii}	74.19 (7)	O7^{ii}—Tb1—O5^{iii}	134.85 (6)
O1—Tb1—O2^{ii}	137.02 (7)	O4^{i}—Tb1—O9	75.43 (6)
O4^{i}—Tb1—O6^{iii}	76.83 (7)	O8—Tb1—O9	137.47 (6)

O8—Tb1—O6^{iii}	83.15 (6)	O1—Tb1—O9	148.18 (6)
O1—Tb1—O6^{iii}	75.05 (6)	O2^{ii}—Tb1—O9	68.08 (6)
O2^{ii}—Tb1—O6^{iii}	128.51 (6)	O6^{iii}—Tb1—O9	105.34 (3)
O4^{i}—Tb1—O7^{ii}	75.18 (9)	O7^{ii}—Tb1—O9	66.05 (6)
O8—Tb1—O7^{ii}	121.85 (7)	O5^{iii}—Tb1—O9	70.41 (4)
O1—Tb1—O7^{ii}	98.28 (8)	O4^{i}—Tb1—O8^{ii}	106.89 (8)
O2^{ii}—Tb1—O7^{ii}	74.83 (7)	O8—Tb1—O8^{ii}	73.31 (8)
O6^{iii}—Tb1—O7^{ii}	151.98 (6)	O1—Tb1—O8^{ii}	70.29 (7)
O4^{i}—Tb1—O5^{iii}	105.13 (7)	O2^{ii}—Tb1—O8^{ii}	73.14 (7)
O4^{i}—Tb1—O8	145.69 (8)	O6^{iii}—Tb1—O8^{ii}	142.12 (5)
O4^{i}—Tb1—O1	73.74 (8)	O7^{ii}—Tb1—O8^{ii}	51.04 (7)

Symmetry codes: (i) 3/2-x, 1/2+y, 1/2-z; (ii) 3/2-x, 1/2-y, 1-z; (iii) 2-x, -y, 1-z.